

# Uncertainty Management in Coupled Physical-Biological Lower-Trophic Level Ocean Ecosystem Models

*Ralph F. Milliff, Sr.*, Research Associate, Cooperative Institute for Research in Environmental Science, University of Colorado, 216 UCB, Boulder, CO 80309-0216, USA;

[milliff@colorado.edu](mailto:milliff@colorado.edu)

*Jerome Fiechter*, Assistant Researcher, Institute of Marine Sciences, University of California, Santa Cruz, CA, USA

*William B. Leeds*, Postdoctoral Fellow, Department of Statistics and Department of Geophysical Sciences, University of Chicago, Chicago, IL, USA

*Radu Herbei*, Assistant Professor, Department of Statistics, Ohio State University, Columbus, OH, USA

*Christopher K. Wikle*, Professor, Department of Statistics, University of Missouri, Columbia, MO, USA

*Mevin B. Hooten*, Assistant Professor, Department of Statistics and Department of Fish, Wildlife and Conservation Biology, Colorado State University, Fort Collins, CO, USA

*Andrew M. Moore*, Professor, Ocean Sciences Department, University of California, Santa Cruz, CA, USA

*Thomas M. Powell*, Professor Emeritus, Department of Integrative Biology, University of California, Berkeley, CA, USA

*Jeremiah L. Brown*, Principal Scientific Group LLC, Fishers, IN, USA

## ABSTRACT

### 1. Introduction

Sources of uncertainty in ocean ecosystem models arise from abstractions necessary to reduce complexity and represent essential ecosystem processes in an aggregate sense. These biogeochemical models are replete with parameters, many of which are poorly known or abstracted from experiments, times and locations that might not be relevant to the ecosystem under study. Moreover, the ocean ecosystem model parameters are correlated in some instances, and in almost all cases ocean ecosystem model parameters do not benefit from an abundance of data. Indeed, uncertainty also arises in the hard-won observations of ecosystem variables; both in terms of measurement error and errors of representativeness. The under-determination problem in parameter specification (e.g. Ward et al., 2010) is an inherent issue in ocean ecosystem model development and interpretation.

The mismatch between sparse information from imperfect observations *versus* many, correlated and imperfectly-defined parameters is well-known to ocean ecosystem modelers. It is the topic of recurring workshops in marine biogeochemical modeling (e.g., see special issue of *Journal of Marine Systems*, 2010) and it has been qualified and quantified in a pioneering feasibility demonstration by Harmon and Challenor (1997), and more recently in papers by Friedrichs and co-workers (e.g., Friedrichs et al., 2007; 2009; Ward et al., 2010), Dowd (e.g., Dowd 2007; 2011), and others (e.g., Malve et al., 2007, Margvelashvili and Campbell, 2012).

Under-determination challenges arose in a study of the coupled physics and biology of the coastal Gulf of Alaska (CGOA), with a focus on the lower-trophic level (LTL) ecosystem response to environmental forcings. Qualification and quantification of under-determination, and ecosystem model parameter estimation were achieved in spite of it. The limitations and success in the CGOA ocean ecosystem parameter estimation process are recounted in this paper. The story involves an interplay between deterministic and probabilistic approaches that provide an update on methodological tools for ocean ecosystem model parameter estimation given under-determination.

### ***Physical-Biological Setting in the CGOA***

General circulation features of the CGOA (Figure 1) include the Alaska Current, entering the domain from the northeast along a narrow shelf offshore of Sitka and Yakutat; and the Alaska Stream, exiting the domain from northeast to southwest along the broad shelf offshore of the Kenai Peninsula, Kodiak Island, and Shumagin Island. Important synoptic scale circulation features include Yakutat eddies that propagate along the shelfbreak in the direction of the Alaska Current and Alaska Stream for several weeks at a time; driving exchanges of shelf and basin waters with important biological implications (Brown and Fiechter, 2012; Fiechter and Moore, 2012).

**<< Figure 1 goes about here >>**

The LTL ecosystem characteristics in the CGOA consist of shelf, shelf-break and ocean basin regimes. The shelf regime is iron rich due to river sources and resuspension of bottom

sediments. Spring bloom dynamics comprise the principal driver for primary production on the shelf. A weaker bloom also occurs in Fall in most years (see Fiechter, 2012 and references therein). With increasing distance off the shelf, the phytoplankton abundance is increasingly limited by iron availability such that the basin waters are a high-nutrient low-chlorophyll (HNLC) regime. The shelf and basin regimes are affected by the Yakutat eddies that propagate slowly along the shelf-break and transport iron-rich shelf waters offshore and nutrient-rich basin waters onshore.

### ***Bayesian Hierarchical Modeling***

We begin from a Bayesian hierarchical model (BHM) perspective. Bayesian modeling is a probabilistic approach wherein random variables are endowed with probability distributions. Following Cressie and Wikle (2011; see also Berliner et al., 2003), we organize the components of a BHM into 3 parts leading to the posterior distribution of interest. Starting with Bayes Theorem, write:

$$[ \mathbf{X}, \theta_p, \theta_d | \mathbf{Y} ] \propto [ \mathbf{Y} | \mathbf{X}, \theta_d ] [ \mathbf{X} | \theta_p ] [ \theta_p ] [ \theta_d ] \quad (1)$$

where the notation  $[ \mathbf{A} ]$  denotes a probability distribution for random variable  $\mathbf{A}$ , and  $[ \mathbf{A} | \mathbf{B} ]$  is the conditional distribution for  $\mathbf{A}$  given  $\mathbf{B}$ . The ocean ecosystem processes of interest (e.g., phytoplankton and zooplankton abundances) are given by  $\mathbf{X}$  and associated observations (e.g., SeaWiFS surface chlorophyll retrievals and zooplankton counts from net tow data) by  $\mathbf{Y}$ . As such, the first term on the right hand side of (1) is the data stage distribution, and the second term is the process model distribution. The  $\theta_p$  and  $\theta_d$  are parameters that arise in specifications of the process and data stage models, and they are assumed here to be independent, completing the right hand side of (1). These right hand side distributions are convolved in a Bayesian solution procedure to obtain estimates of the posterior probability distribution of interest; i.e., the left hand side of (1), where the posterior includes estimates for the distributions of the process  $\mathbf{X}$  and parameters  $\theta_p, \theta_d$ ; given the data  $\mathbf{Y}$ . The data stage and process model distributions in (1) represent these BHM components at the highest level of the model hierarchy. An essential part of BHM

strategy is to condition distributions for complex (joint) processes that are difficult to specify, on component processes for which data exist and/or model formulations are more certain. Sources of uncertainty are similarly conditioned and specified, process-by-process and observation type-by-observation type, down the model hierarchy. In this way, uncertainty management is explicitly built into BHM design.

In our CGOA application the process ( $\mathbf{X}$ ) is the time-dependent abundances of state variables in a six-compartment LTL ocean ecosystem model to be described. Process model parameters ( $\theta_p$ ) are given by a subset of the many parameters of the LTL ocean ecosystem model. Data ( $\mathbf{Y}$ ) are taken from: a) time-averaged surface chlorophyll retrievals from SeaWiFS data in the CGOA; and b) nutrient and phytoplankton concentrations from vertical profiles taken, onshore and offshore of the shelf break, at GLOBEC stations in the CGOA (Figure 1). The data stage parameters ( $\theta_d$ ) include measurement error estimates for SeaWiFS and the GLOBEC Station data.

Fiechter et al. (2009; 2013) describe a deterministic version of the LTL ocean ecosystem model adapted to the BHM in the CGOA. The differential equations and parameter definitions for the LTL model are reproduced from Fiechter et al. (2013) in Tables 1 and 2. The model includes state variables for dissolved nitrogen, phytoplankton biomass, zooplankton biomass and detritus (i.e. NPZD, with time-dependent abundances given in units of nitrogen concentration), as well as dissolved iron and phytoplankton-associated iron given in terms of iron concentration. Extensions of the traditional NPZD model are incorporated to: a) address iron limitation effects on primary production in offshore waters of the CGOA (so, an NPZDFe LTL ocean ecosystem model); and b) include a vertical mixing term parameterized by mixed-layer depth in each of the state variable equations.

### ***Estimating the Posterior Distribution***

According to (1), there is at least the hope that, given sufficient data ( $\mathbf{Y}$ ), distributions for the NPZDFe model parameters ( $\theta_p$ ) could be updated and available in the posterior distribution. But how much data is sufficient? What kinds of data are optimal? And what

are the underlying issues that complicate parameter estimation in the NPZDFe BHM? To put these issues in context, we first need to review (in words) the procedures for estimating the posterior distribution in the BHM.

Equation (1) is expressed as a proportionality. To form an equality, the right hand side of (1) is divided by an integral over all possible states of the observations and processes such that the posterior distribution on the left hand side of (1) is a proper probability distribution. The normalizing integral term is intractable in large state and parameter space problems of the kinds characterized by an ocean ecosystem BHM. Instead, estimates of the posterior distribution are obtained by Monte Carlo methods in sampling algorithms that have been adapted to higher-dimension problems. Initial values are taken for a subset of the process model parameters to be treated as random variables, and updated in the posterior distribution. Through the NPZDFe process model, the fixed and random parameters define an initial state for the ocean ecosystem. Proposal parameters are then selected in a Markov process wherein random perturbations from the previous values are obtained. The implied state vector is computed and compared with the previous state and current observations. Depending on the outcome of the state comparison, the new set of parameters are either accepted and become the latest entries in the estimate of the posterior distribution for  $\theta_p$ , or they are rejected and the frequency of occurrence for the previous set of parameters is incremented by one in the posterior estimate. This is an outline of the Metropolis-Hastings (M-H) algorithm that forms the basis of many Markov-Chain Monte Carlo (MCMC) methods to estimate posterior distributions in BHM. Useful practical implementations of M-H algorithms depend on efficient proposals such that all important regions of parameter space are visited and acceptance rates are around 25%.

MCMC sampling can be thought of in an analogy with descent algorithms that are perhaps more familiar to deterministic modelers (i.e. in the solution of elliptic operators that arise in data assimilation and primitive equation solvers). The dimension of the state and parameter space in the BHM is tied to the number of random variables. The ranges over which perturbations from the initial values are selected bound the iteration space for

MCMC sampling. Efficient sampling occurs when the M-H algorithm explores local and global extrema in the fewest feasible number of iterations (analogous to finding gradients in steepest descent algorithms). Conversely, if random variables are correlated and conditional distributions for the data do not project upon distributions for specific parameters or state variables, the solution surface is smooth and local extrema are very hard to identify and explore efficiently by iteration.

In the statistics parlance, “Bayesian learning” expresses the extent to which the convolution of distributions on the right hand side of (1) can update the distributions for state variables in  $\mathbf{X}$  and parameters in  $\theta_p$ . If the data stage distribution does not project upon regions of the process model distribution the updates do not change initial distributions and the process and/or parameters do not exhibit learning relative to the prior specification of the process model distribution. Expanding data types and/or reducing the set of random variables in the BHM design might serve as remedies, but these changes are often infeasible (i.e. in the case of expanded observations for ocean ecosystem parameters), or only achieved by trial and error. Remedies of these kinds were explored in the NPZDFe BHM for the CGOA as described below. This notion of Bayesian learning is related to the statistical notion of “identifiability.” We say that a parameter is identifiable if, given enough information, it is theoretically possible to learn the value of that parameter. Thus, in this article we will say that a parameter that does not exhibit Bayesian learning is not identifiable.

### ***Initial BHM Experiments***

The NPZDFe equations in the Table 1 include O(20) parameters; far too many to be identified by the relatively sparse datasets from SeaWiFS retrievals and the GLOBEC stations. We started with six random parameters for the NPZDFe process model (i.e. the  $\theta_p$ ). They were (see Table 2): the phytoplankton maximum growth rate ( $V_{mNO3}$ ), the half-saturation constant for iron (KFeC), the initial slope of the phytoplankton-light utilization curve (PhyIS), the maximum grazing rate for zooplankton consumption of phytoplankton (ZooGR), the remineralization rate for detritus (DetRR), and the fraction of the available

iron that is remineralized (FeRR). Initial values for these parameters in the CGOA were taken from the deterministic coupled physical-biological model calculations described by Fiechter et al. (2009). Ranges over which random perturbations to the initial values could be selected in the M-H algorithm were the subjects of experimentation, but sensible estimates were provided by expert opinion and published values.

Tables 1 and 2 (reproduced from Fiechter et al., 2013) demonstrate that the parameters treated as random variables in our BHM enter the NPZDFe LTL ocean ecosystem model affecting phytoplankton abundance. These are sensible choices for the random parameters of the BHM since most of our data stage information will also be related to phytoplankton abundance. However, the correlations among some of these parameters, and the number of parameters relative to the sparse data, result in M-H acceptance rates well below 25% and parameters that are not identifiable by the data. This latter point is crucial in the interpretations of the posterior distribution from the BHM to be described.

## **2. Ensemble Calculations in a Coupled Physical-Biological Extension of the Regional Ocean Modeling System in the CGOA**

To learn more about the parameter under-determination in the NPZDFe BHM application in the CGOA, we turned to deterministic tools. An ensemble of forward-model calculations (Fiechter, 2012) was run in the coupled physical-biological model for the CGOA developed by Fiechter, Moore and co-workers (Fiechter et al., 2009; Fiechter and Moore, 2009; Fiechter et al., 2011). The coupled model system for the CGOA is comprised of a physical model component that is the Regional Ocean Modeling System (ROMS; Haidvogel et al., 2008) and a LTL ecosystem model component that is a six-compartment augmentation of an NPZD model with 2 additional compartments for iron remineralization and phytoplankton associated iron concentration; i.e. NPZDFe. As noted above, this biological model component is also the basis of the process model in the BHM. Coupled physical-biological forward model calculations in the CGOA with the deterministic system use best estimates for the 19 parameters of the biological model component. Some of these parameters are well known and/or independent of regional specifics. Others are relatively

unknown in the CGOA and based on estimates from other regions (e.g. a California Current System study by Powell et al., 2006). Coupled model simulations successfully reproduce seasonal variability in LTL ecosystem response (Fiechter et al., 2009) as well as signals associated with synoptic eddies in the CGOA (Brown and Fiechter, 2012; Fiechter and Moore, 2012).

Ensemble calculations with the coupled biological-physical model are designed to provide a set of state variable responses to parameter variations. Fiechter (2012) reports ensemble calculations with the coupled biological-physical model for the CGOA for 2001; a year that included strong Spring and weaker Fall phytoplankton blooms on the shelf and an interaction with a Yakutat eddy off the shelf-break in Summer. Seven biological parameters were varied for each forward model ensemble member according to Latin Hypercube randomizations given reasonable ranges around the parameter values from control runs (e.g. Fiechter et al., 2009). The perturbed parameters included: the initial slope of the light utilization curve by phytoplankton (PhyIS); the maximum growth rate for phytoplankton ( $V_{mNO3}$ ); the half-saturation constant for nitrogen ( $K_{NO3}$ ); the half-saturation constant for iron ( $K_{FeC}$ ); the zooplankton grazing rate (ZooGR); and remineralization rates for detritus (DetRR) and iron (FeRR). These parameters directly affect the equation for phytoplankton abundance (see Tables 1 and 2) and they overlap the set of parameters treated as random variables in the initial experiments with the BHM.

The state variable simulations for phytoplankton,  $P$ , in each ensemble member, are compared with 8-day average surface phytoplankton retrievals from SeaWiFS to begin to identify key biological parameters and confirm biological scenarios for the LTL ecosystem evolution on synoptic and seasonal timescales in the CGOA. The ensemble approach is limited by the costs of the coupled physical-biological calculation for each ensemble member, and by the extent to which the biological model parameter space is explored by the perturbations from control values in a few parameters.

Fiechter (2012) also examined the effects of ensemble size and parameter range variations on the summaries obtained from the ensemble experiments. The leading spatial empirical

orthogonal function (EOF) pattern, the associated amplitude time series, and the ensemble spreads in each, for surface chlorophyll concentrations in 2001 were insensitive to ensemble sizes of 25 members and above. They were more sensitive to increasing ranges supplied to the Latin Hypercube algorithm for randomization of the 7 biological parameters; with minimum spread when the parameter ranges were  $\pm 10\%$  of the respective control values, and maximum spreads for parameter ranges spanning values from half to double the control values. Greater range in the biological parameters led to an earlier phytoplankton bloom in Spring (by up to 3 weeks). Agreement with 8-day average surface phytoplankton concentration retrievals from SeaWiFS was also insensitive to ensemble size, but sensitive to parameter range in the ensemble experiments. The best agreement with averaged SeaWiFS occurred for the half-double parameter range constraint. These agreements were best during the Spring bloom on the shelf. Target diagrams that locate every ensemble member in a root-mean-square-difference vs. bias (i.e. model – observations) space were plotted for comparisons with the 8-day average surface chlorophyll as well. The target diagrams help identify particular ensemble members (i.e. a specific set of parameter values) that minimize differences and bias.

To identify parameter impacts in sub-domains of the CGOA Fiechter (2012) performed multivariate linear regressions for the surface chlorophyll concentration given terms representing each of the 7 biological parameters that were randomly perturbed for each ensemble member. Each regression coefficient (one for each parameter) identifies the relative impact (in a normalized least squares sense) of its associated biological parameter. The random parameters explaining the largest fractions of the variance in surface phytoplankton concentration are weighted by the largest normalized regression coefficients.

To isolate temporal variability in the leading parameters, the linear regression analysis was spatially averaged over shelf and basin regions of the CGOA for 25-member ensembles when the parameter values spanned ranges from half to double the default values. Figure 2 depicts the normalized monthly average regression coefficient for each parameter for the period March through October 2001 from Fiechter (2012). The left panel shows the

correlations on the shelf and the right panel the relative impacts in the CGOA basin. On the shelf, primary production in the Spring bloom is consistent with efficient utilization of sunlight and rapid phytoplankton growth; i.e. large amplitude normalized regression coefficients for PhyIS and VmNO<sub>3</sub>. PhyIS is again important leading into the Fall bloom. P abundance is moderated by zooplankton, Z, grazing in Summer and Fall as noted by large negative normalized regression coefficients in ZooGR for May-October. While bloom signals for the basin regime are similar in PhyIS, VmNO<sub>3</sub> and ZooGR, there are additional important terms having to do with uptake of dissolved iron by phytoplankton cells (KFeC) and iron remineralization (FeRR).

<< **Figure 2 goes about here** >>

When the spatial-averaging is relaxed, point-by-point linear regressions can be used to identify spatial distributions of the dominant normalized regression coefficients, and therefore biological parameters, in the LTL ecosystem of the CGOA. Figure 3 depicts maps of dominant biological parameters contributing to P abundance for 3 seasons of 2001; May, July and September, representing the Spring bloom, the Summer synoptic eddy season and the Fall bloom. We discuss here the results for the 25-member ensemble given half-double ranges in the 7 biological parameters. For comparisons involving many ensemble sizes and parameter ranges see Fiechter (2012).

The dominant ecosystem process on the shelf in April is the Spring bloom and the controlling parameter is PhyIS over most of the shelf. Offshore, the ecosystem is iron-limited and this is reflected in the importance of the half saturation constant for dissolved iron uptake, K<sub>FeC</sub>. By Summer, ZooGR controls the P abundance on the shelf in the middle of the domain and across the shelf break into the basin over most of the domain. The light-limitation parameter, PhyIS, is negatively correlated with sustaining primary productivity into Summer in nearshore regions; i.e. less efficient light utilization preserves some nutrients for later in the year. Remineralization of iron (FeRR) plays a dominant role offshore and in the south. There is a hint of nutrients being drawn off the shelf in the north where a spatial patch on the scale of a Yakutat eddy is dominated by the VmNO<sub>3</sub> parameter. This corresponds to an eddy location noted in Brown and Fiechter (2012) and

Fiecther and Moore (2012). By Fall, ZooGR controls P abundance from the coast across the shelf break in the south, while signals of the Fall bloom due to DetRR and PhyIS are evident onshore in the north. Dominant parameters in the basin are similar to the Summer distributions with FeRR in the south, KeFC in the north, and evidence of onshore-offshore transports along the shelf break where PhyIS and ZooGR are most important.

<< **Figure 3 goes about here** >>

The ensemble calculations have identified seasonal, synoptic and sub-domain variabilities in dominant parameters of the LTL ecosystem dynamics for the CGOA up to the limits explored in terms of ensemble size and ranges in the subset of biological parameters (i.e. 7 of 19) varied in the experiments. Randomly selected parameter values led to surface phytoplankton estimates that could be compared with 8-day and monthly averages from SeaWiFS retrievals. For the purposes of parameter probability distribution estimation, the ensemble experiments have identified a few key parameters and suggested reasonable ranges to pose as priors for  $[\theta_p]$  in (1).

### **3. The Parameter-Estimation BHM in the CGOA**

The NPZDFe BHM was revisited in light of the insights gained from ensemble calculations in the coupled physical-biological forward model. The 1-D vertical BHM was implemented at inner and outer shelf locations on the GLOBEC line off the Kenai Peninsula (Fig. 1) during 2001. The NPZDFe process model is unchanged from the earlier implementation and the data stage inputs are taken separately and in combinations from: surface phytoplankton retrievals from daily SeaWiFS data; temporally intermittent *in-situ* observations of nitrate and chlorophyll at the GLOBEC stations; and from coupled physical-biological model output to be used for sensitivity tests and validation experiments. We focus on 2001 because concurrent measurements of nitrate and chlorophyll are available at both the inner and outer shelf GLOBEC stations that year in April, May and July (Strom et al., 2006). The inner shelf location is representative of nitrate-limited primary production with strong Spring and weaker Fall blooms in P. The outer shelf location is offshore of the shelf break where

iron limitation is important and P abundance does not exhibit a strong seasonal signal. To demonstrate parameter estimation in the NPZDFe BHM, we highlight a few interpretations and implications from the posterior distribution estimates obtained, with a focus on the inner shelf location. For a more complete analysis, including equal emphasis on posterior distribution estimates for the outer shelf location, see Fiechter et al., 2013.

We begin with 2 random parameters;  $VmNO_3$  and  $ZooGR$ , shown to be important in controlling P abundance in the ensemble calculations.  $VmNO_3$  is the most flexible parameter to reflect the full range of potential phytoplankton growth rates.  $PhyIS$  was important in setting the onset of the Spring bloom, but its functional dependence (i.e., as the coefficient for the light limitation term) is limited to the range  $[0,1]$  as are other terms (e.g., Michaelis-Menten nutrient limitation) in the equation governing phytoplankton growth (see Tables 1 and 2). Also, recall that in the NPZDFe BHM a vertical mixing term based on mixed-layer depth estimates refines the timing of the Spring bloom onset. So, we revisit the NPZDFe BHM with  $VmNO_3$  and  $ZooGR$  as random parameters, while fixing the other parameters (Table 2) at their default values.

The NPZDFe BHM can be validated in part by replacing *in-situ* and remotely-sensed data stage inputs with simulated observations from the control run of the coupled physical-biological model. These are so-called “nearly perfect data experiments”. The goal is to reproduce in the posterior distribution of the NPZDFe BHM the default values used in the forward model for the random parameters  $VmNO_3$  and  $ZooGR$ . The simulated data in these experiments are “nearly perfect” because there is no explicit account in the 1-D BHM for the time-dependent 3-D effects of the ocean circulation in and around the GLOBEC stations that does affect P in the forward model. The nearly-perfect data experiments did reproduce, with negligible spread, posterior mean values for  $VmNO_3$  and  $ZooGR$  thereby validating the implementation of the NPZDFe BHM and indicating that 3-D circulation effects on P were secondary (Fiechter et al., 2013).

The nearly perfect data sampling was degraded in time and content to study the effects of more realistic data stage inputs and to help interpret posterior distributions from NPZDFe

BHM experiments using SeaWiFS and GLOBEC station data stage inputs. Inferences regarding sampling that emerge from these sensitivity studies include (Fiechter et al., 2013): a) it is important to capture data, both for the onset (i.e., dominated by P growth) and decay (i.e., controlled by Z grazing) phases, of the Spring bloom on the shelf; b) *in-situ* samples of more than one state variable (e.g. chlorophyll and nitrate) usefully constrain posterior distributions of interest; and c) data stage inputs with widely different space-time properties (e.g. resolution, seasonality, vertical vs. surface biases in coverage, etc.) might not be additive in their contributions to refining posterior distribution estimates.

<<< **Figure 4 goes about here** >>>

Figure 4 shows estimates of the posterior distributions for VmNO<sub>3</sub> (top row) and ZooGR (bottom row) for the inner shelf location when degraded forward model outputs (denoted ROMS NPZDFe in Fiechter et al., 2013) are used as data stage inputs in the BHM to mimic the temporal and vertical sampling and data types collected at the GLOBEC station (left column), SeaWiFS sampling (middle column) and combined GLOBEC and SeaWiFS sampling (right column). Large uncertainty in VmNO<sub>3</sub> for GLOBEC sampling of forward model output is shown by Fiechter et al. (2013) to be due to the absence of station data in the early phases of the Spring bloom. The uncertainty in VmNO<sub>3</sub> is greatly reduced using forward model output with SeaWiFS sampling intervals and the same is true for combined GLOBEC and SeaWiFS (right column). The SeaWiFS sampling covers the initial phases of the Spring bloom. ZooGR is well estimated given forward model data stage inputs for all sampling intervals. Zooplankton grazing does not control P abundance until after the peak in the Spring bloom on the shelf (e.g. see Fig 3).

When the real *in-situ* GLOBEC station data and SeaWiFS remote sensing data are used in isolation and in combination (Figure 5), the posterior distribution estimates for VmNO<sub>3</sub> and ZooGR at the inner shelf location are more complicated. Vertical profiles of nitrate and chlorophyll from the GLOBEC station data are sufficient to estimate posterior mean values for VmNO<sub>3</sub> and ZooGR that are close to default values with very little uncertainty. However, the posterior distribution estimates using SeaWiFS-only data stage inputs are

farther from the default values. There is evidence of noise in the posterior for  $VmNO_3$  that Fiechter et al. (2013) attribute to high-frequency variability in the SeaWiFS data that is missing in smoother forward model output (See Fig 4). Posterior distribution estimates for ZooGR using SeaWiFS-only data stage inputs exhibit an as yet unexplained bi-modality with modal values much larger than the default values. The combined GLOBEC and SeaWiFS data lead to a posterior distribution estimate for  $VmNO_3$  that is highly uncertain, while the bi-modality in ZooGR disappears and the posterior mean value is closer to the default. Recall that SeaWiFS provides an estimate of chlorophyll only at the surface, averaged over a 10km area. The GLOBEC station data include profiles of chlorophyll and nitrate at 10m intervals in the vertical. Apparently, these datasets are detecting different processes affecting P abundance at the GLOBEC inner shelf station location.

<<< **Figure 5 goes about here** >>>

Identifiability issues begin to arise when the number of random parameters is expanded to 6. Figure 6 shows the posterior distribution estimates for (from left) PhyIS,  $VmNO_3$ , ZooGR, DetRR, KFeC and FeRR at the inner shelf location given GLOBEC station data (top row), SeaWiFS surface chlorophyll retrievals (middle row) and the combined GLOBEC and SeaWiFS data (bottom row). These data stage inputs to the NPZDFe BHM now identify 6 random parameters controlling P abundance limitations due to light, nitrogen, iron and remineralizations of detritus and iron. Individual datasets (either GLOBEC or SeaWiFS) lead to posterior distributions exhibiting significant uncertainties for almost all parameters. In the GLOBEC data stage input case the uncertainty in  $VmNO_3$  noted in the 2 random parameter BHM has been compensated in some sense by a low but relatively certain distribution for PhyIS. Low values of the light limitation parameter are offsetting large but uncertain values in growth rate. The compensation appears to go the other way (i.e. large and uncertain PhyIS and lower but relatively certain  $VmNO_3$ ) in the SeaWiFS only data stage case that focuses on surface chlorophyll only. This is an example of parameter correlation making the interpretation of ecosystem dynamics from BHM output more challenging. Note that in the 6 random parameter BHM, combining datasets reduces uncertainty in the posterior distributions for all parameters; with many parameter

posterior mean values near default values. The exception is FeRR which was not shown to be important on the shelf in the ensemble experiments (Fiechter, 2012; see also Figs 2, 3).

<<< **Figure 6 goes about here** >>>

<<< Possible Box: What does iron limitation look like in 2 and 6 random parameter BHMs?

Careful consideration of the posterior distribution estimates for the parameters of the NPZDFe BHM can be used to: quantify identifiability; evaluate differing information content in differently sampled data stage inputs; and qualify ecosystem dynamical interpretations (i.e. in terms of certainties). Validation and sensitivity experiments with simulated data stage inputs from skillful forward model integrations are essential to diagnosing these issues as well (i.e. the nearly-perfect-data experiments). However, computational costs associated with many thousands of iterations through the M-H algorithm constrain the number of experiments that can be run. Limitations in the abundance and precision of data stage inputs constrain the number of parameters that can be treated as random and identified in the posterior. These constraints preclude BHM experiments wherein random parameters are identified in space (i.e. at each grid point or in sub-regions on the shelf, shelf-break or in the basin) and time (i.e. for different phases of the Spring bloom). In the next section, we describe developments to circumvent computational costs such that many more degrees of freedom enter the Bayesian analysis.

#### **4. Bayesian Statistical Emulators for Estimating Parameters and State Variables**

The use of statistical “emulators” or “surrogates” to approximate complex deterministic forward models has seen increasing use in recent years, particularly in model calibration (i.e. procedures for inferring parameters; e.g., Kennedy and O'Hagan, 2001; Higdon et al, 2008; Rougier, 2008). This is often accomplished in a two-stage approach. In the first stage, emulators are constructed by running the forward model under multiple different input (calibration) parameter settings. Then, some summary measure of the forward model output is considered a response surface relative to the input parameters, and a covariance-based statistical model (e.g., a Gaussian Process model) is used to “fill in” the output surface

so that one predicts the forward model (summary) output at untried input settings. In the second stage, if real-world observations are available that correspond to the response surface summary variable, then these statistical models can be estimated with classical or Bayesian methods, and provide a reasonable calibration of the forward model.

We used statistical emulators to help facilitate uncertainty quantification of the CGOA NPZDFe and CGOA ROMS-NZPDFe models. In particular, we evaluated parameter uncertainty of the CGOA-NPZDFe model, linked one-dimensional (vertical) NPZDFe models across spatial locations, and assimilated both models with SeaWiFS observations to obtain complete spatial fields of near surface phytoplankton. The emulator-based solutions to these problems are described briefly below. Critical to our methodology is the use of what we have labeled “first-order” emulators, which differ from the response surface approach described above in that our focus is on modeling the response through its mean (e.g., first-order moment; Hooten et al., 2011) rather than covariance (second-order moments) based approaches which rely on Gaussian Processes (GPs).

### ***First-Order Emulator-Assisted Parameter Estimation***

**<<< Figure 7 goes about here >>>**

Hooten et al. (2011) showed that one can obtain parameter estimates for complicated nonlinear forward models by the use of first-order emulator approximations within a Bayesian estimation approach. The key to this approach is that the forward model output is obtained for a subset of scientifically plausible parameter values. Then, one develops a statistical model to describe the input-output relationship. A critical component of the modeling is that the dimensionality of the model output is reduced through a truncated singular value decomposition of the forward model output. The right singular vectors are modeled statistically in terms of the forward model inputs as well as some statistical parameters. This relationship is formulated in the context of a nonlinear statistical model, with associated additive errors, and the associated statistical model parameters are estimated “off-line” from the forward model output. Given actual observations corresponding to the model output, and a prior distribution for the forward model input parameters, the posterior distribution of these parameters can be obtained without having

to re-run the forward model. This procedure is illustrated graphically in Figure 7 and in the following steps:

1. Select sets of 7 randomized input parameters,  $\theta_{p1}, \dots, \theta_{pK}$  (i.e. from the prior distribution  $[\theta_p]$ ).
2. For  $\theta_{pi}$  run the forward model  $f(\theta_{pi}, \gamma)$  (where  $\gamma$  corresponds to ancillary model input such as boundary and initial conditions and “fixed” parameters), obtaining the desired output vector  $x_i$ .
3. Collect output into matrix  $X = (x_1, \dots, x_K)$ .
4. Perform singular value decomposition of the matrix in step 3 to get  $X = UDV'$  and approximate it by a subset of left and right singular vectors; i.e.  $X \approx \tilde{U}\tilde{D}\tilde{V}'$ .
5. Develop a statistical model for each right singular vector with  $\theta_{pi}$  as a predictor variable corresponding to response variable  $v_i$  in the  $i^{th}$  column of  $\tilde{V}$ . The resulting statistical model is  $v(\theta, \hat{\beta})$ , where  $\hat{\beta}$  are the estimated statistical model parameters.
6. Perform model calibration, using  $\tilde{U}\tilde{V}v(\theta^*, \hat{\beta})$  in place of  $f(\theta^*, \gamma)$ .

Hooten et al. (2011) applied this procedure to a 50-member ensemble of the ROMS-NPZDFe coupled physical-biological model of the CGOA. In this experiment, 7 of the 19 biological parameters were allowed to vary randomly from a truncated normal distribution with scientifically plausible lower and upper bounds and location parameter equal to the default value for the parameter. The first-order emulator was constructed based on the first three singular vectors (accounting for approximately 99% of the variability in the ensemble) and a random forest model was used to estimate the relationship between the right singular vectors and the input parameters. The additive error was included through a bootstrapping approach based on random sampling of predictive residuals. The input parameters were given uniform prior distributions over the scientifically plausible range of variation. To evaluate the ability to recover true parameter values where the only model uncertainty comes from the use of a statistical surrogate, the Bayesian estimation procedure was run 50 times, each time assuming that one ensemble member was the observed “truth” and using the other 49 ensemble members to construct the emulator. This study showed that certain parameters could be recovered, but not all (an example of the

under-determination problem). These results were corroborated when we used actual SeaWiFS observations as well (which introduces model structural uncertainty as well as measurement uncertainty).

### ***Modeling 3-D Processes with a Forest of 1-D Emulators***

Biogeochemical model parameters can vary in space (e.g., Friedrichs et al. 2007; see also Fig. 3). It is plausible to link a series of 1-D NPZDFe models through a 2-D spatial field on their parameters in order to characterize the rough 3-D structure of biogeochemical process. In particular for the CGOA, the dynamics behave differently along the inner shelf, the outer shelf and in the synoptic eddy corridor, yet the variability is more similar along the shelf regions and in the eddy corridor. Given the successful implementation of the first-order emulator in the coupled ROMS-NPZDFe case, we investigated the possibility of linking several 1-D NPZDFe models (a “forest of 1-D models”) through a hierarchical model that linked the parameters (Leeds et al. 2012b). Critically, rather than doing this directly with the NPZDFe models, we used the first-order emulator implementation of the 1-D models in our BHM. The model input parameters were then given spatially-dependent prior distributions that respected the anisotropic dependence across and along shelf.

The model was implemented to investigate two spatially varying parameters corresponding to the zooplankton grazing rate, ZooGR, and the half-saturation constant for iron, KFeC. Data were from SeaWiFS. Both parameters showed evidence of Bayesian learning given the data and the spatial linkage was more critical for the than ZooGR.

<<< **Figure 8 goes about here** >>>

### ***Emulator-Assisted Biogeochemical Data Assimilation***

It is also plausible to develop statistical emulators for the dynamical operators in forward models (e.g., Conti et al., 2009). Traditionally, such implementations have not considered knowledge related to the inherent nonlinear interactions that are present in complicated environmental and ecological processes. We developed a BHM that incorporated a parametric nonlinear emulator to perform data assimilation of near-surface phytoplankton and the coupled ROMS-NPZDFe model along with SeaWiFS observations. In particular, our

model considers the interaction of sea surface temperature (SST), sea surface height (SSH), and phytoplankton (P) fields through time (Leeds et al. 2012a).

A key component of this model is the representation of the multivariate spatial field (SST, SSH, P) as the sum of a lower dimensional dynamical process and a lower-dimensional (multivariate spatial) non-dynamical process. This can be accomplished naturally in the context of the first-order emulator procedure by considering the higher-order singular vectors to correspond to the time-varying dynamical process and allowing the remaining singular vectors to correspond to the non-dynamical component. One then models the evolution of the right singular vectors through a nonlinear evolution operator. In our case, we utilized the parametric quadratic nonlinear model of Wikle and Hooten (2010) because it explicitly accounts for dyadic nonlinear interactions.

The emulator was developed with 8-day averages of ROMS-NPZDFe SSH, SST, and P output for 1998-2001. The BHM was then run given SeaWiFS ocean color observations for 2002 in place of the ROMS-NPZDFe phytoplankton output. As shown in Figure 8, the model was able to blend the ROMS-NPZDFe dynamics with the observations in a framework that provides realistic measures of assimilation uncertainty.

## **5. Summary**

The interplay between deterministic and probabilistic methods leads to clearer understanding of LTL ecosystem dynamics in the CGOA and the extent to which those dynamics are conditioned upon key parameters of the ecosystem model. The quantification of uncertainty through in the posterior distribution of the BHM is an incremental advance in understanding at the abstracted level of the NPZDFe LTL ecosystem model approximation. In addition to these specific results, much of the work here can be considered a “proof-of-methodology” as well. The refinement of the NPZDFe BHM and the specific focus on key parameters of the LTL ecosystem model in the BHM (Fiechter et al., 2013), depend upon intuition gained in ensemble experiments in the coupled physical-biological forward model (Fiechter, 2012). Limitations in the state-space

dimension tractable in the BHM are overcome by constructing Bayesian emulators based on leading space-time patterns deduced from, again, ensemble forward model calculations (Hooten et al., 2011). In the larger state-space Bayesian emulator applications, parameters borrow strength in horizontal spatial dimensions such that estimates for parameters are obtained for shelf, shelf-break and basin sub-regions of the CGOA domain (Leeds et al., 2012b). Bayesian emulators are also used to provide estimates, with space and time-variable uncertainties, for surface P fields from sparse and imperfect SeaWiFS observations (Leeds et al., 2012a).

In general, the under-determination problem is not going away. Although we have relatively large amounts of satellite-derived estimates of near surface phytoplankton abundance from the ocean color proxy, these observations are incomplete and fairly uncertain. The NPZDFe models considered here are abstractions of more complicated multi-component LTL ocean ecosystem models (e.g., NEMURO). The identifiability issues discussed here are only going to be amplified in these more complicated models. This suggests that uncertainty quantification in biogeochemical models will be focused on the relatively few identifiable parameters, or the focus will change to one of state prediction rather than parameter inference. In this case, there is a great need to account for the uncertainties in these predictions and to use these predictive distributions to link to other higher trophic levels of the ocean ecosystem. A major use of these linkages will be to study both the consequences of management decisions and global climate change. The major components of these models are likely to include stochastic parameterizations or emulator-based processes. Both approaches will require significant contributions from statistical scientists in collaboration with physical and biological oceanographers. We believe that the results presented here provide a template for how such collaborations can be achieved.

#### *ACKNOWLEDGEMENTS*

## References

- Berliner, L.M., R.F. Milliff and C.K. Wikle, 2003: Bayesian hierarchical modeling of air-sea interaction., *Journal of Geophysical Research*, **108**(C43104), doi:10.1029/2002JC001413.
- Brown, J.L. and J. Fiechter, 2012: Quantifying eddy-chlorophyll covariability in the coastal Gulf of Alaska.. *Dynamics of Atmospheres and Oceans*, **55-56**, 1-21, doi:10.1016/j.dynatmoce.2012.04.001.
- Conti, S., J. Gosling, J. Oakley and A. O'Hagan, 2009: Gaussian process emulation for dynamic computer codes., *Biometrika*, **96**(3), 663-676.
- Cressie, N. and C.K. Wikle, 2011: **Statistics for Spatio-Temporal Data**, *Wiley Series in Probability and Statistics*, John Wiley and Sons, Inc., 588pgs.
- Dowd, M., 2007: Bayesian statistical data assimilation for ecosystem models using Markov Chain Monte Carlo., *Journal of Marine Systems*, **68**, 439-456.
- Dowd, M., 2011: Estimating parameters for a stochastic dynamic marine ecological system., *Environmetrics*, **22**, 501-515.
- Fiechter, J., R. Herbei, W. Leeds, J. Brown, R. Milliff, C. Wikle, A. Moore and T. Powell, 2013: A Bayesian parameter estimation method applied to a marine ecosystem model for the coastal Gulf of Alaska., *Ecological Modelling*, **258**, 122-133.
- Fiechter, J., 2012: Assessing marine ecosystem model properties from ensemble calculations., *Ecological Modelling*, **242**, 164-179.
- Fiechter, J., G. Broquet, A.M. Moore and H.G. Arango, 2011: A data-assimilative, coupled physical-biological model for the coastal Gulf of Alaska., *Dynamics of Atmospheres and Oceans*, doi:10.1016/j.dynatmoce.2011.01.002.
- Fiechter, J., A.M. Moore, C.A. Edwards, K.W. Bruland, E. DiLorenzo, C.V.W. Lewis, T.M. Powell, E.N. Curchitser and K. Hedstrom, 2009: Modeling iron limitation of primary production in the coastal Gulf of Alaska., *Deep Sea Research II*, **56**(2503), doi:10.1016/j.dsr2.2009.02.010.
- Fiechter, J. and A.M. Moore, 2009: Interannual spring bloom variability and Ekman pumping in the coastal Gulf of Alaska., *Journal of Geophysical Research*, **114**, C06004, doi:10.1029/2008JC005140.
- Fiechter, J. and A.M. Moore, 2012: Iron limitation impact on eddy-induced ecosystem variability in the coastal Gulf of Alaska., *Journal of Marine Systems*, **92**, 1-15, doi:10.1016/j.jmarsys.2011.09.012.
- Friedrichs, M.A.M. et al., 2007: Assessment of skill and portability in regional marine biogeochemical models: Role of multiple planktonic groups., *Journal of Geophysical Research*, **112** (C08001), doi: 10.1029/2006JC003852.
- Friedrichs, M., Dusenberry, J., Anderson, L., Armstrong, R., Chai, F., Christian, J., Doney, S., Dunne, J., Fujii, M., Hood, R., McGillicuddy, D.J., Moore, J.K., Schartau, M., Sptiz, Y.H., Wiggert, J.D., 2007: Assessment of skill and portability in regional marine biogeochemical models: role of multiple planktonic groups., *Journal of Geophysical Research*, **112**, 1-22.
- Friedrichs, M.A.M, et al., 2009: Assessing the uncertainties in model estimates of primary productivity in the tropical Pacific Ocean., *Journal of Marine Systems*, **76**, 113-133.
- Haidvogel, D.B., et al., 2008: Ocean forecasting in terrain-following coordinates: formulation and skill assessment of the Regional Ocean Modeling System., *Journal of Computational Physics*, **227**, 3595-3624, doi:10.1016/j.jcp.2007.06.016.

- Harmon, R. and P. Challenor, 1997: A Markov chain Monte Carlo method for estimation and assimilation into models., *Ecological Modelling*, **101**, 41-59.
- Higdon, D., J. Gattiker, B. Williams and M. Rightly, 2008: Computer model calibration using high-dimensional output., *Journal of the American Statistical Association*, **103**(482), 570-583.
- Hooten, M.B., W.B. Leeds, J. Fiechter and C.K. Wikle, 2011: First-order emulator inference for parameters in nonlinear mechanistic models., *Journal of Agricultural, Biological and Environmental Statistics*, **16**(4), 475-494, doi:10.1007/s13253-011-0071-7.
- Kennedy, M. and A. O'Hagan, 2001: Bayesian calibration of computer models., *Journal of the Royal Statistical Society, Series B*, **63**(3), 425-464.
- Leeds, W.B., C.K. Wikle and J. Fiechter, 2012a: Emulator-assisted reduced-rank ecological data assimilation for nonlinear multivariate dynamical spatio-temporal processes, *Statistical Methodology*, doi:10.1016/j.statmet.2012.11.004.
- Leeds, W.B., C.K. Wikle, J. Fiechter, J.L. Brown and R.F. Milliff, 2012b: Modeling 3-D spatio-temporal biogeochemical processes with a forest of 1-D statistical emulators., *Environmetrics*, **24**(1), 1-12, doi:10.1002/env.2187.
- Malve, O., M. Laine, H. Haario, T. Kirkkala and J. Sarvala, 2007: Bayesian modeling of algal mass occurrences- using adaptive MCMC methods with a lake water quality model., *Environmental Modelling and Software*, **22**, 966-977.
- Margvelashvili, N. and E.P. Campbell, 2012: Sequential data assimilation in fine-resolution models using error-subspace emulators: Theory and preliminary evaluation., *Journal of Marine Systems*, **90**, 13-22, doi:10.1016/j.jmarsys.2011.08.004.
- Moore, A.M., H.G. Arango, G. Broquet, B.S. Powell, J. Zavala-Garay and A.T. Weaver, 2011: The Regional Ocean Modeling System (ROMS) 4-Dimensional variational data assimilation systems, Part I: System overview and formulation., *Progress in Oceanography*, **91**, 34-49, doi:10.1016/j.pocean.2011.05.004.
- Powell, T.M., C.V.W. Lewis, E.N. Curchitser, D.B. Haidvogel, A.J. Hermann and E.L. Dobbins, 2006: Results from a three-dimensional nested, biological-physical model of the California Current System and comparisons with statistics from satellite imagery., *Journal of Geophysical Research*, **111**(C0), 7018, doi:10.1029/2004JC002506.
- Rougier, J., 2008: Efficient Emulators for Multivariate Deterministic Functions., *Journal of Computational and Graphical Statistics*, **17**(4), 827-843.
- Strom, S.L., M. Brady Olson, E.L. Macri and C.W. Mordy, 2006: Cross-shelf gradient in phytoplankton community structure, nutrient utilization and growth rate in the coastal Gulf of Alaska., *Marine Ecology Progress Series*, **328**, 75-92.
- Ward, B.A., M.A.M. Friedrichs, T.R. Anderson and A. Oschlies, 2010: Parameter optimization techniques and the problem of underdetermination in marine biogeochemical models., *Journal of Marine Systems*, **81**, 34-43, doi:10.1016/j.jmarsys.2009.12.005.
- Wikle, C.K. and M.B. Hooten, 2010: A general science-based framework for spatio-temporal dynamical models., *Test*, **19**, 417-451.

## Tables

<b>NPZDFe Lower Trophic Ecosystem Model</b>	
Dissolved nitrogen:	$\frac{\partial N}{\partial t} = \delta D + \gamma_n GZ - UP + \kappa \frac{\partial^2 N}{\partial z^2}$
Phytoplankton:	$\frac{\partial P}{\partial t} = UP - GZ - \sigma_d P + \kappa \frac{\partial^2 P}{\partial z^2}$
Zooplankton:	$\frac{\partial Z}{\partial t} = (1 - \gamma_n)GZ - \xi_d Z + \kappa \frac{\partial^2 Z}{\partial z^2}$
Detritus:	$\frac{\partial D}{\partial t} = \sigma_d P + \xi_d Z - \delta D + w_d \frac{\partial D}{\partial z} + \kappa \frac{\partial^2 D}{\partial z^2}$
P-associated iron:	$\frac{\partial F_p}{\partial t} = F_p \left( U - \frac{GZ}{P} - p_m \right) + L_{Fe} + \kappa \frac{\partial^2 F_p}{\partial z^2}$
Dissolved iron:	$\frac{\partial F_d}{\partial t} = F_p \left( f_{rem} \left( \frac{GZ}{P} + p_m \right) - U \right) - L_{Fe} + \kappa \frac{\partial^2 F_d}{\partial z^2}$
Phytop. growth rate:	$U = \frac{R^2}{R^2 + k_{Fe}^2} \frac{V_m N}{k_N + N} \frac{\alpha I}{\sqrt{V_m^2 + \alpha^2 I^2}}$
Phytop. iron uptake:	$L_{Fe} = \frac{R_0 - R}{t_{Fe}} P [C : N]$
Empirical and realized [Fe:C] ratios:	$R_0 = b F_d^a, \quad R = \frac{F_p}{P [C : N]}$
Light availability at depth:	$I = I_0 \exp \left( k_z z + k_p \int_0^z P(z') dz' \right)$
Zooplankton growth rate:	$G = R_m \left( 1 - e^{-\Lambda P} \right)$
Vertical mixing term:	$\kappa \sim MLD_{ROMS} \text{ (} MLD = \text{Mixed Layer Depth)}$

Table 1. Biological source and sink terms for the 1-D NPZDFe model and growth functions for phytoplankton and zooplankton (see Table 2 for parameter definitions and values).

Parameter Name	Symbol	Value	Units
<b>Light</b>			
Light extinction coefficient	$k_z$	0.067	$\text{m}^{-1}$
Self-shading coefficient	$k_p$	0.04	$\text{m}^2 \text{mmolN}^{-1}$
<b>Phytoplankton</b>			
Initial slope of P-I curve ( <i>PhyIS</i> )	$\alpha$	0.02	$\text{m}^2 \text{W}^{-1}$
Maximum uptake rate ( <i>VmNO3</i> )	$V_m$	0.8	$\text{day}^{-1}$
Nitrogen half-saturation constant	$k_N$	1.0	$\text{mmolN m}^{-3}$
Half-saturation for [Fe:C] ( <i>KFeC</i> )	$k_{Fe}$	16.9	$\text{mmolFe (molC)}^{-1}$
Empirical [Fe:C] power	$a$	0.6	nondimensional
Empirical [Fe:C] coefficient	$b$	64	$(\text{mmolC m}^{-3})^{-1}$
Iron uptake time scale	$t_{Fe}$	1.0	day
Mortality	$\sigma_d$	0.1	$\text{day}^{-1}$
<b>Zooplankton</b>			
Maximum grazing rate ( <i>ZooGR</i> )	$R_m$	0.4	$\text{day}^{-1}$
Ivlev constant	$A$	0.84	nondimensional
Excretion efficiency	$\gamma_n$	0.3	nondimensional
Mortality	$\zeta_d$	0.145	$\text{day}^{-1}$
<b>Remineralization</b>			
Detritus remin. rate ( <i>DetRR</i> )	$\delta$	0.2	$\text{day}^{-1}$
Detritus sinking	$w_d$	8.0	$\text{m day}^{-1}$
Iron remin. fraction ( <i>FeRR</i> )	$f_{rem}$	0.5	nondimensional

Table 2. Parameter names, symbols, values, and units for the 1-D NPZDFe model. Parameters treated as random in the BHM framework are indicated in bold italics (i.e., *PhyIS*, *VmNO3*, *ZooGR*, *DetRR*, *KFeC*, *FeRR*).

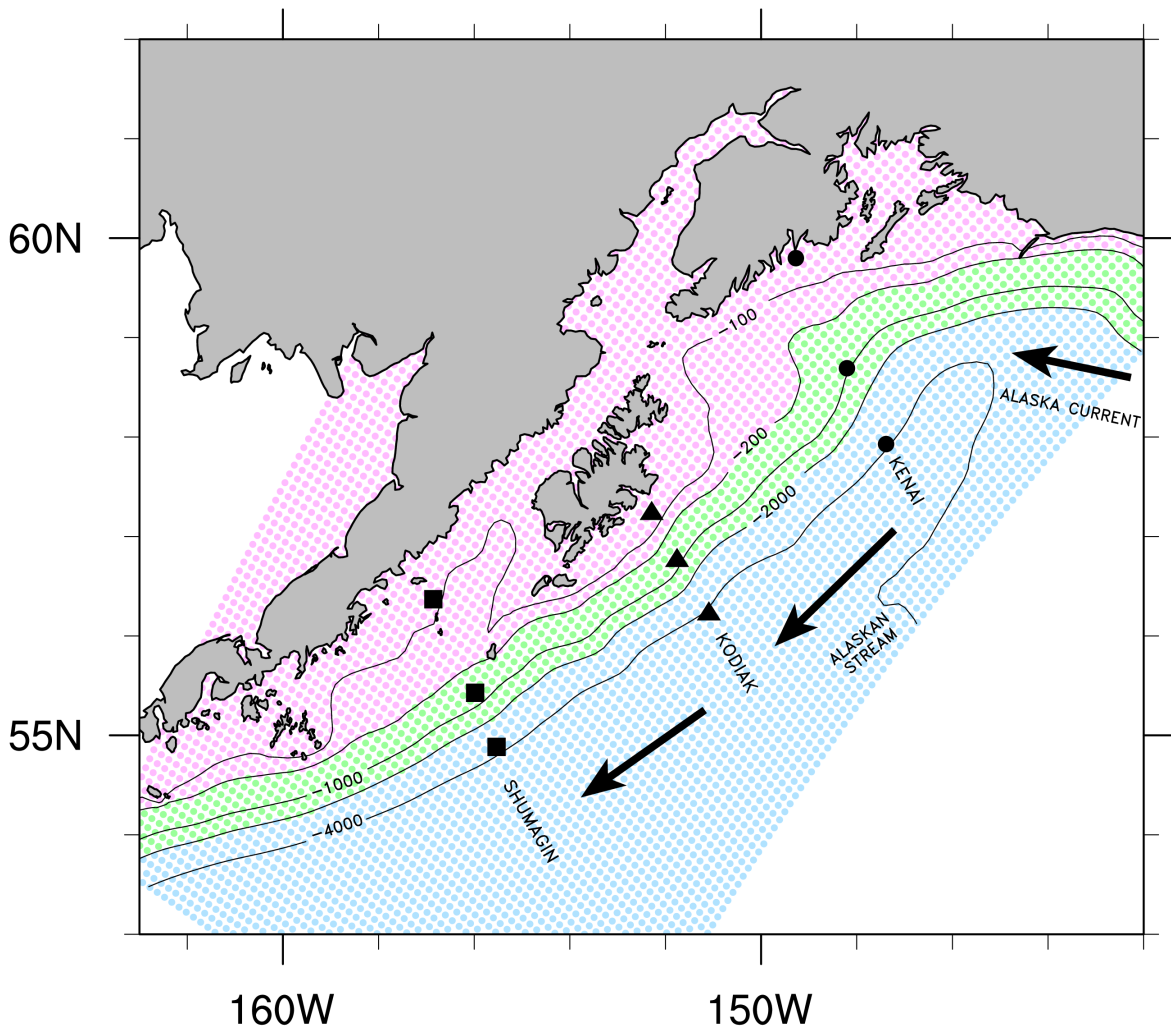


**Figure 1.** Coastal Gulf of Alaska (CGOA) domain (adapted from Leeds et al., 2012b). GLOBEC stations along the Kenai, Kodiak and Shumagin lines are noted. Each line consists of an inner shelf, outer shelf and offshore station. The shelf break is indicated by the 200m, 1000m and 2000m isobaths. Directions for the general circulation features; Alaska Current and Alaska Stream are indicated.

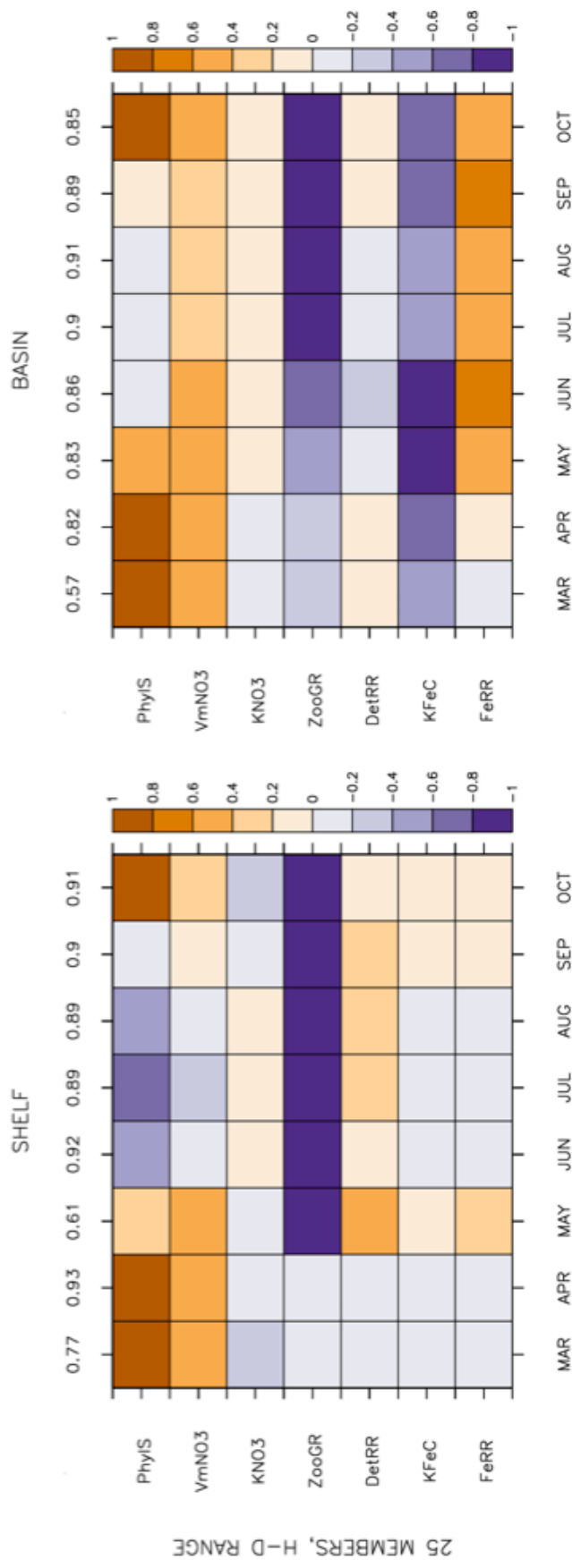


**Figure 2.** Normalized regression coefficients for LTL ecosystem model parameters (vertical axes) vs. month in 2001 (horizontal axes) for shelf (left) and basin (right) sub-regions of the CGOA domain. A multivariate linear regression for surface phytoplankton concentration was spatially averaged (shelf and basin) for all ensemble members wherein the LTL ecosystem model parameters were randomly perturbed over the range of half-to-double of the default values. Regression coefficients are normalized by the largest value for each parameter across all ensemble members. Adapted from Fiechter et al., 2013.

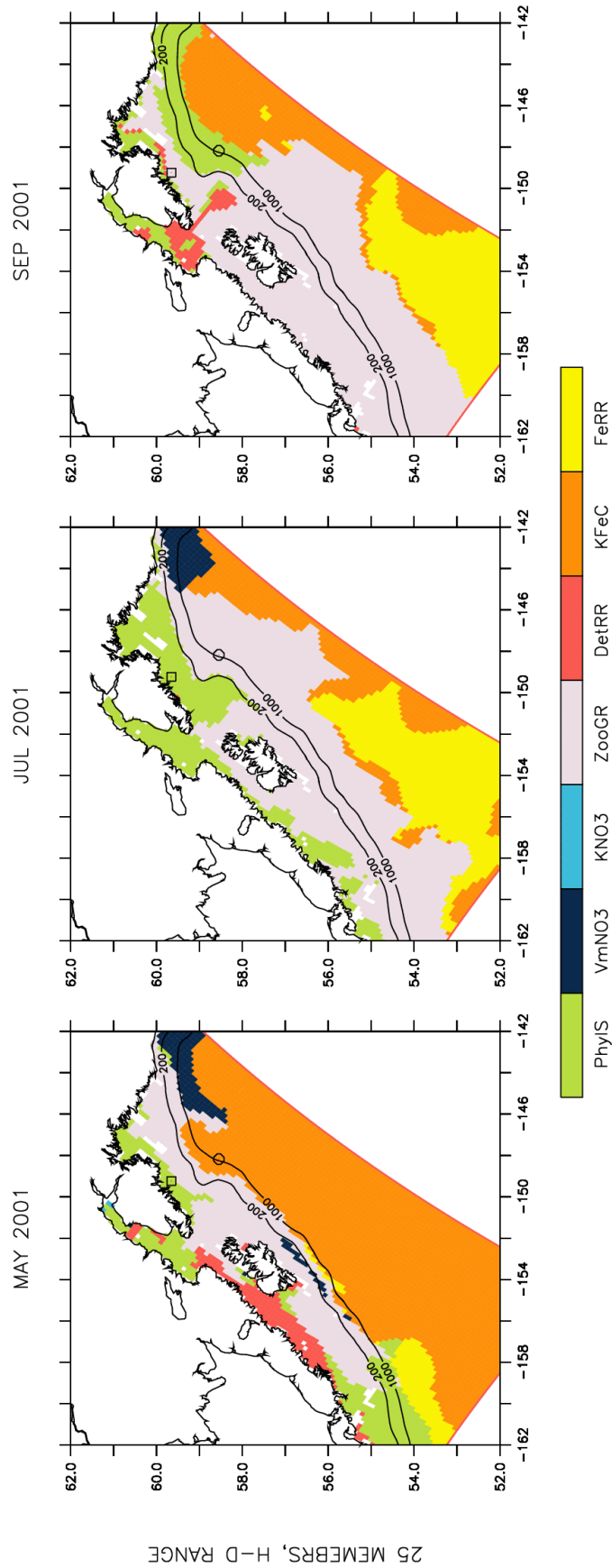


**Figure 3.** Largest-amplitude normalized regression coefficients for LTL ecosystem model for three seasons in 2001. A multivariate linear regression for surface phytoplankton concentration was computed for each surface location in the CGOA domain, for all ensemble members wherein the LTL ecosystem model parameters were randomly perturbed over the range of half-to-double the default values. Regression coefficients are normalized by the largest value for each parameter across all ensemble members. Adapted from Fiechter et al., 2013.

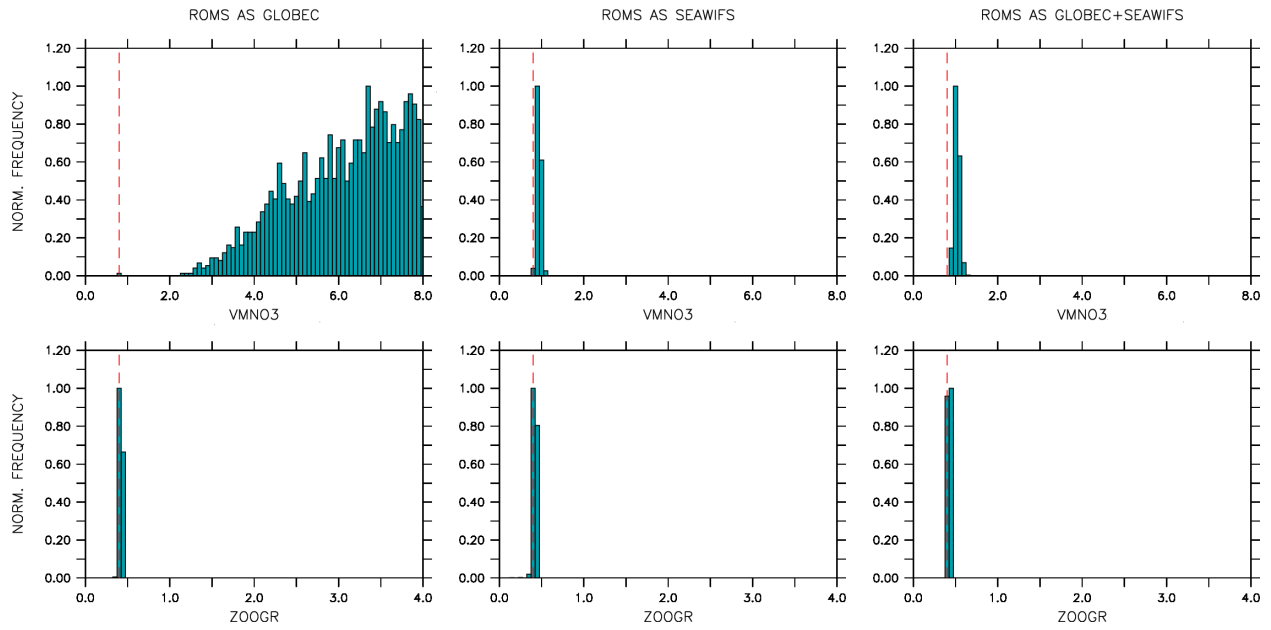


**Figure 4.** CGOA Inner-shelf posterior distributions for phytoplankton growth rate (VmNO3; top) and zooplankton grazing rate (ZooGR; bottom) using ROMS-NPZDFe subsampled as GLOBEC (left), SeaWiFS (center) and both (right) as data stage. Dashed vertical red lines indicate default parameter values (see Table 2).

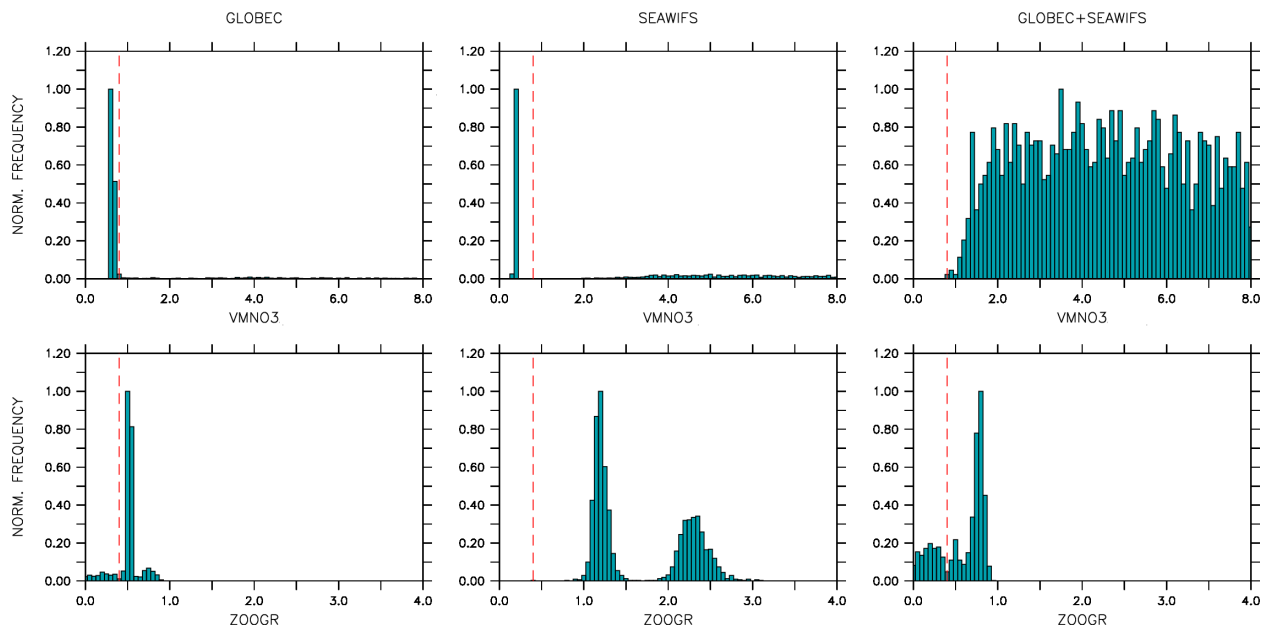


**Figure 5.** CGOA Inner-shelf posterior distributions for phytoplankton growth rate ( $V_{mNO3}$ ; top) and zooplankton grazing rate ( $ZooGR$ ; bottom) using observations from GLOBEC (left), SeaWiFS (center) and both (right) as data stage. Dashed vertical red lines indicate default parameter values (see Table 2).

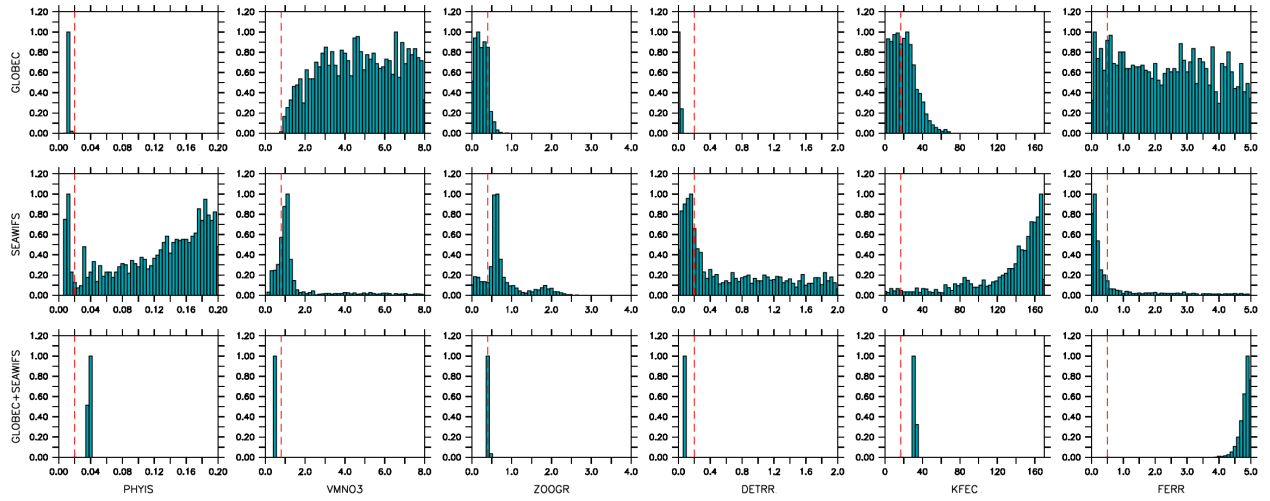


**Figure 6.** CGOA Inner-shelf posterior distributions for PhyIS, VmNO<sub>3</sub>, ZooGR, DetRR, KFeC and FeRR (from left to right) using observations from GLOBEC (top), SeaWiFS (middle) and both (bottom). Dashed vertical red lines indicate default parameter values (see Table 2).

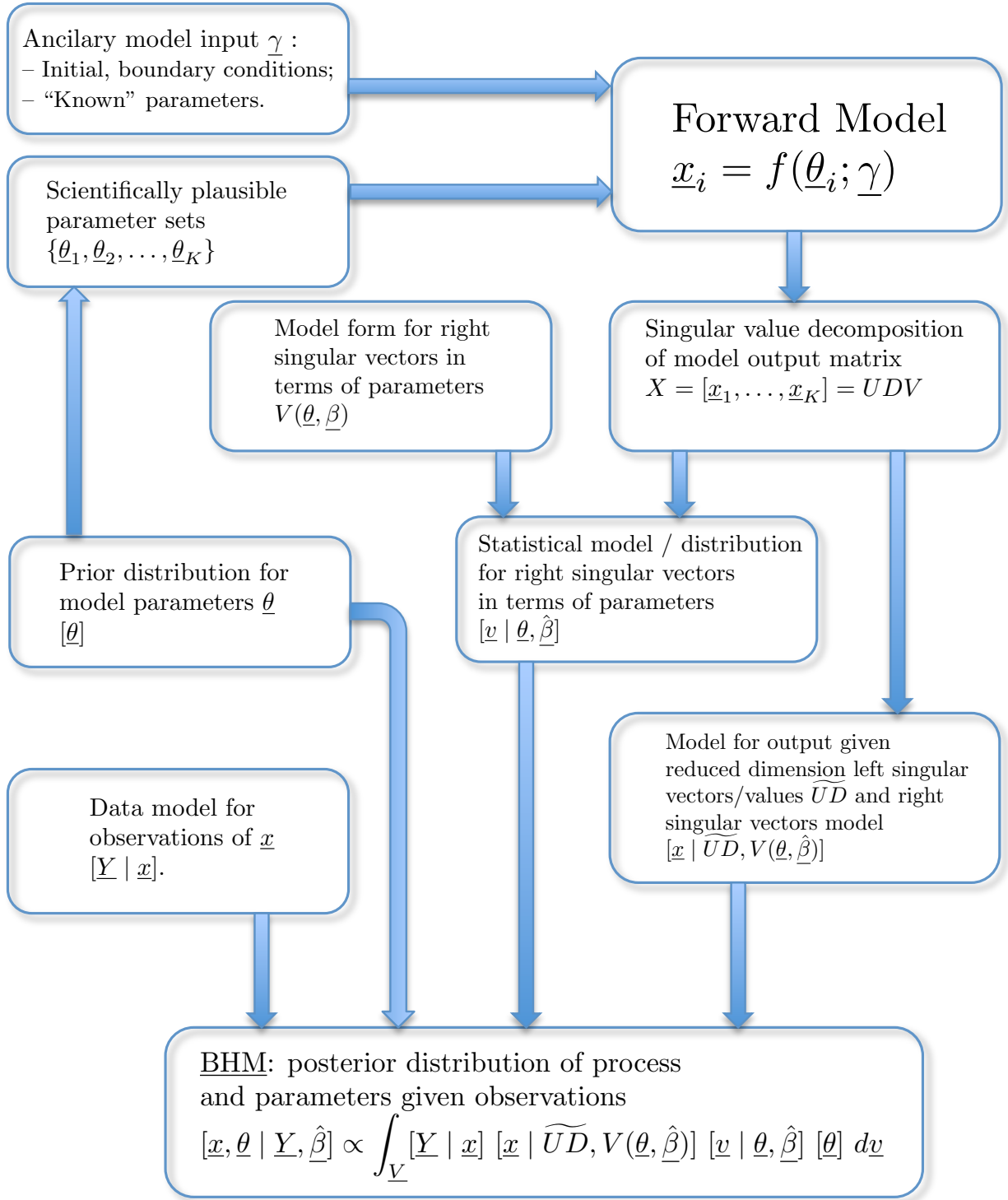


**Figure 7.** Bayesian emulator flow-chart (see text).

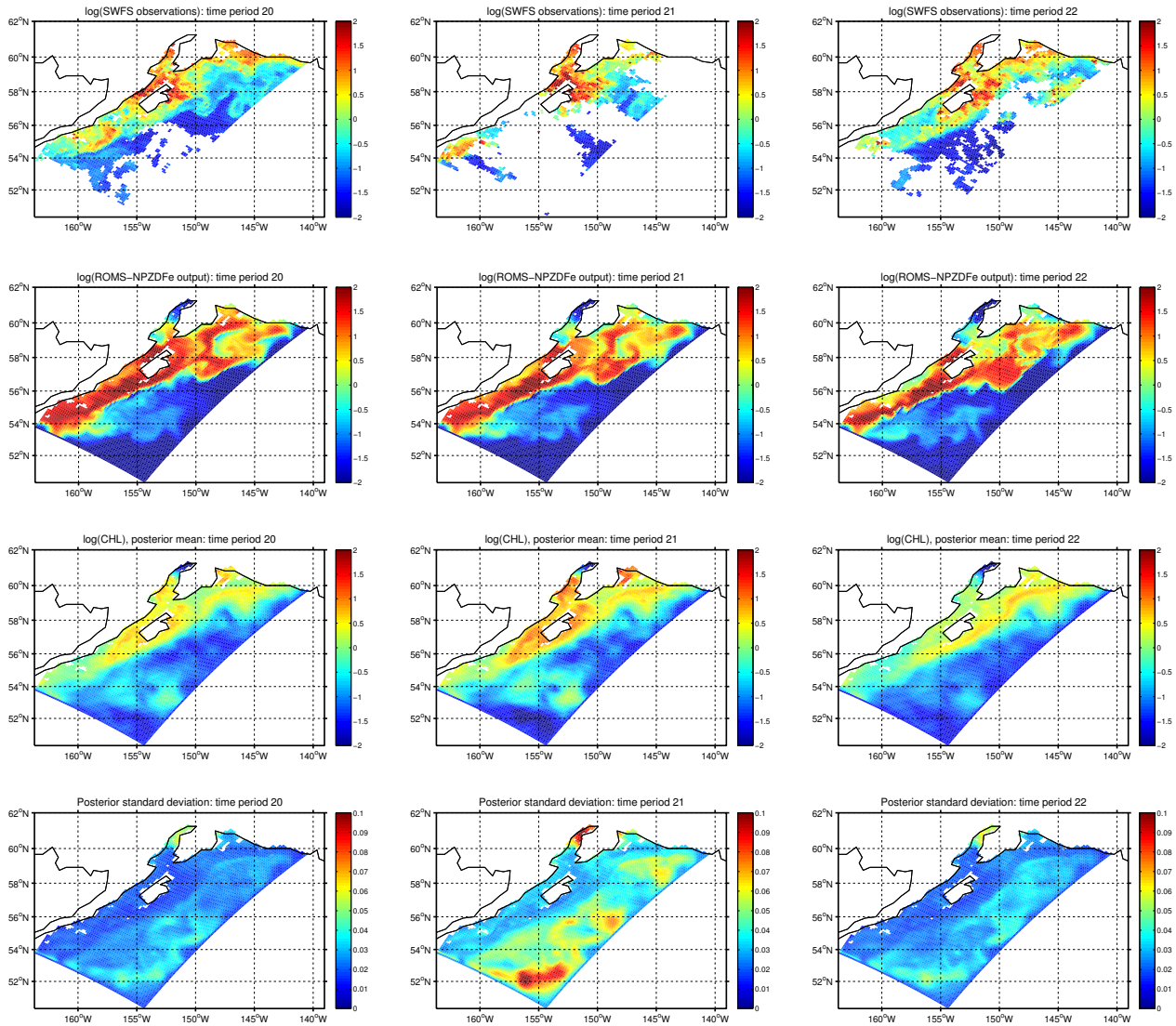


**Figure 8.** Plots of log-transformed SeaWiFS ocean color observations (top row), ROMS-NPZDFe phytoplankton output (second row), posterior mean (third row), and posterior standard deviation (fourth row), for three eight-day time periods: June 2, 2002 to June 9, 2002 (left column), June 10, 2002 to June 17, 2002 (center column), and June 18, 2002 to June 25, 2002 (right column). Adapted from Leeds (2012a).